Applied Acoustics 242 (2026) 111060

Contents lists available at ScienceDirect

Applied Acoustics

journal homepage: www.elsevier.com/locate/apacoust

A hybrid strategy of OTPA and machine learning for efficient root-cause analysis of NVH in multi-source systems

Sharif Khakshournia [a], Shaygan Shahed Haghighi [a], Marzie Majidi [a], Farhad Najafnia [a], Hamed Haddad Khodaparast [b,*]

[a] Noise and Vibration Department, Automotive Industries Research & Innovation Center of SAIPA (AIRIC), Tehran, Iran
[b] Faculty of Science and Engineering, Swansea University, Bay Campus, Fabian Way, Swansea, Crymlyn Burrows SA1 8EN, United Kingdom

ARTICLE INFO

Keywords:
Operational transfer path analysis
Random forest
NVH diagnosis
Sensitivity analysis
Machine learning
Contribution analysis

ABSTRACT

The growing awareness of health benefits, along with the competitive emphasis on vehicle comfort, has led automakers to place greater attention on reducing Noise, Vibration, and Harshness (NVH). One of the most beneficial techniques for NVH engineers to identify, rank, and eliminate dominant noise and vibration sources and paths is Transfer Path Analysis (TPA). Unlike traditional TPA, Operational Transfer Path Analysis (OTPA) requires neither the preliminary acquisition of the transfer matrix between excitation and response points nor the measurement of forces transferred through the active and passive side connection points. Although the OTPA method offers significant advantages over classical TPA methods, it still faces challenges such as data loss caused by the pseudo-inversion of the indicator matrix. In this paper, we estimate the transmissibility matrix using a machine learning-based regression algorithm (random forest). We demonstrated that machine learning is an effective alternative to the truncated Singular Value Decomposition (SVD) method for estimating the transmissibility matrix, as it is a swift solution that preserves essential information in the indicator matrix. The efficiency of the method has been verified by a 2.28 % improvement in the Sound Pressure Level (SPL) of the driver's ear noise of a sedan-type vehicle through the modification of the most critical path found by this approach.

1. Introduction

As automotive technologies evolve with electric powertrains and new structural design concepts, accurate identification and ranking of noise sources become increasingly crucial to address emergent or previously insignificant sources. Pinpointing and ranking the primary noise and vibration sources and paths in vehicles are pivotal for effective mitigation strategies. The development of advanced analytical techniques enables manufacturers to precisely identify the specific components or mechanisms that contribute most significantly to interior noise and vibration across relevant frequency bands. This targeted approach allows focused efforts on addressing root causes rather than attempting broad-based symptomatic solutions. These analytical methods, such as Transfer Path Analysis (TPA) and contribution analysis, empower manufacturers to stay ahead of evolving customer expectations for refinement and comfort while ensuring compliance with stringent noise regulations [1–3].

TPA-based methods analyze propagation of noise and vibration, from the excitation source in the active subsystem to the target point in passive subsystems, through paths in a complex system. Classical TPA methods depict the passive subsystem response and the influences of source excitation on the target point via the interface forces between the active and passive subsystems [4]. Hence, the method requires the interface forces acting during operational conditions and then Frequency Response Functions (FRFs) of the passive subsystem. Despite its apparent simplicity, the technique faces some several significant challenges [5,6]. First, determination of operational interface forces while the system is assembled becomes challenging, since mounting force-transducers between passive and active subsystems is impractical. Another challenge is the necessity to disassemble the passive and active subsystems to measure passive side FRFs, which leads to inaccurate responses, along with technical difficulties.

Component-based Transfer Path Analysis (CB-TPA) is another method that characterizes the excitation forces of an active component

* Corresponding author.
E-mail addresses: Khakshournia.s@airic-ir.com (S. Khakshournia), majidi.m@airic-ir.com (M. Majidi), najafnia.f@airic-ir.com (F. Najafnia), H.Haddadkhodaparast@Swansea.ac.uk (H.H. Khodaparast).

https://doi.org/10.1016/j.apacoust.2025.111060
Received 22 January 2025; Received in revised form 27 August 2025; Accepted 4 September 2025

independently from the entire system, allowing engineers to isolate the source of noise and vibration. Unlike classical TPA, which depends on the assembled dynamics and requires a new operational test for each design modification, CB-TPA uses equivalent forces or velocities that are inherent properties of the active component itself. This enables more flexible NVH predictions by applying these forces to the system's FRFs after the active part is shut down, thus providing an accurate analysis of different subsystems without the need for reassembly [4]. In this regard, Almirón et al. [7] used CB-TPA to successfully predict vehicle interior noise from rolling tires, demonstrating the utility of this method in predicting mention vehicle road noise, with applications in tire test-rig measurements and early-stage vehicle development. Bianciardi et al. [8] validated CB-TPA method's application in road noise assessment by combining individual component models with fully assembled system FRFs, thus streamlining the vehicle design process.

To avoid the difficulties associated with determining FRFs in classical TPA and CB-TPA, Noumura and Yoshida [9] proposed using transmissibility function to obtain structure-borne and airborne sound contributions in a vehicle's interior noise during normal operation. Further investigations [10,11] on sound pressure in a vehicle cabin highlighted the advantages of transmissibility function and operational data to reduce the cost and enhance the accuracy of TPA methods. These efforts led to OTPA, which along with Operational Path Analysis with eXogenous input (OPAX) [12] forms the transmissibility- based TPA methods. This category describes energy propagation through a "response-response" relationship between target points and indicator points close to the connection or sources, rather than the more common "excitation-response" relationship. Consequently, the need to dismantle subsystems and explicit force determination to illustrate the role of different paths in energy propagation is eliminated. Meanwhile, reported cases of OTPA application have highlighted its simultaneous benefits and challenges [13,14]. Despite the potential advantages of OTPA method, there are some limitations to its practical implementation including mathematical difficulties. Correlation between signals causes rank deficiency and it makes matrix inversion complex. A typical solution to handle rank deficiency is application of truncated SVD which neglects small singular values and may lead to information loss and misidentification of dominant transfer paths.

In addition to common challenges faced by TPA methods, complex and elaborate designs for modern vehicles highlight the need for more efficient and powerful next-generation TPA-based methods. With the remarkable advancements in data analysis and Machine Learning (ML) techniques, the automotive industry can now benefit from versatile tools to address this need. These modern approaches offer data-driven and statistical solutions that harness the power of large datasets, leverage advanced signal processing algorithms, effectively circumvent inaccuracies and difficulties, enable comprehensive modeling, and provide more accurate predictions [15–17]. In case of TPA, challenges associated with intrusive force measurements during operation, modelling of intricate non-linearities and complex system interactions, accurate source ranking and contribution analysis for effective noise and vibration mitigation strategies can be addressed utilizing these methods.

Recent advances in applying ML and Neural Networks (NN) to conduct TPA has attracted considerable interest. ML approaches primarily perform as a means to replace costly experimental methods with computational approaches and improve accuracy. In this context, three key studies, highlighting the potential of data-driven and statistical solutions for the automotive NVH problems are reviewed: Tsokaktsidis et al. [18] modelled noise transfer in a full vehicle context, using operational measurements from steering systems and cabin microphones. They employed Artificial Neural Networks (ANNs) with REctified Linear Unit (ReLU) and swish activation functions to predict spectral system responses and sensitivities. Addressing the issues of the "dying ReLU" phenomenon and the significance of balanced datasets enabled Mean Absolute Errors (MAE) between 2.94 and 5.37 dB for the studied system. However, data imbalance caused by high-speed operational conditions remained unaddressed.

Later, Lee and Park [19] introduced Deep Neural Networks (DNNs) with fully connected and convolutional layers to model transfer functions from interfacial joints to responses. They enhanced robustness by incorporating phase and cross-spectrum augmentation. Despite successfully matching classical TPA accuracy while eliminating cross-coupling effects for a two-plate test structure, the method requires large datasets. Moreover, results are sensitive to hyperparameters.

The field advanced by the introduction of a physics-driven neural network-based OTPA (NOTPA) [20]. This approach employed Complex-Valued Neural Networks (CVNNs) with identity activation functions. Therefore, it preserved phase information and avoid arbitrary biases, ensuring the derived transmissibility reflected actual vibroacoustic mechanisms. When employed on a box-car structure, the proposed method achieved a lower Mean Absolute Percentage Error (MAPE) than conventional OTPA. It also matched classical TPA in identifying dominant transfer paths, especially at peak frequencies.

These studies share the application of operational data (accelerometers and microphones measurements) instead of requiring additional FRF measurements, in common. While they address distinct issues including rank deficiency, cross-coupling effects, and data imbalance, all highlight the necessity for model optimization and real-world validation.

The present study aims to address the mathematical limitations of conventional OTPA—particularly those related to pseudo-inversion and SVD-induced information loss—by integrating ML algorithms as a robust data-driven alternative. The incorporation of ML is particularly justified due to the underlying physics of TPA, which provides a more nuanced understanding of how noise and vibration propagate through a system. Firstly, this ML-enhanced approach enables analysis of large datasets collected from comprehensive OTPA tests that capture all necessary data in a single iteration, such as a long random drive. Moreover, application of statistical techniques bypasses the need for matrix inversion, thereby avoiding concerns regarding information loss. Traditional transmissibility estimation requires matrix inversion. To handle singularity in matrix inversion process, truncated SVD method is typically utilized. The method truncates singular values below a predetermined threshold. This may lead to information loss and misidentification of dominant transfer paths. On the other hand, making use of the inherent features of the interested case during model designing could prevent unnecessary complexity and reduce computational cost. Thus, the presented approach exploits the linear nature of TPA. By leveraging the principles of TPA, ML algorithms facilitate more accurate identification of noise and vibration sources while minimizing the need for multiple tests or invasive measurements. The proposed methodology is validated through a case study on an SP100-type vehicle, where it successfully identifies and mitigates interior noise issues with high precision, demonstrating that this advanced approach is superior to conventional methods.

The paper is organized into several sections, starting with the Introduction. Section 2 presents an overview of the fundamental concepts of OTPA methods and key implementation considerations. It explores the theoretical and practical cons and pros of OTPA to highlight its significance in the field of NVH analysis. Section 3 introduces the ML-enhanced OTPA approach (ML-OTPA) including applied algorithm, required steps and its potentials to address limitations of conventional OTPA. This section portrays ML-OTPA advantages in terms of efficiency and accuracy. Then, application of a real-world automotive case, demonstrating ML-OTPA effectiveness in source identification, and noise reduction is presented in Section 4. Finally, Section 5 concludes the study, highlighting the method's promising potential as a fast, cost-effective, and highly accurate solution in automotive NVH analysis.

Given the inherent challenges of OTPA and growing demand for efficient NVH root cause analysis on one hand, and the promising outcomes observed in the investigated real case on the other, the proposed method has the potential to contribute to the development of more

reliable noise mitigating strategies.

2. OTPA method

2.1. Theory

The transmissibility concept provides an efficient method to evaluate the contribution and ranking of paths in the response signal during operational system mode. Eliminating the need for subsystems dismounting and FRF calculations reduce the amount of data and cost to an optimal threshold. To define transmissibility, we assume an indicator point, Node 4 with n Degrees of Freedom (DOFs), located close to the interface on the passive subsystem. Indicator point response, $[\mathbf{Y}_4]_{n\times 1}$, caused by source excitations during an operational test, $[\mathbf{X}_1]_{o\times 1}$, is:

$$\mathbf{Y}_4 = \mathbf{H}_{41}^{AB}\mathbf{X}_1 \tag{1}$$

Since $[\mathbf{H}_{41}^{AB}]_{n\times o}$ is a non-square matrix, it does not have an inverse. However, if the rank of n-by-o $\mathbf{H}_{41}^{AB}$ is equal to o, while $o \le n$, then $\mathbf{H}_{41}^{AB}$ is full-rank, and there is a left o-by-n pseudo-inverse matrix $\mathbf{H}_{41}^{AB\ +}$. This guarantees the observability of the excitation DOFs from the indicator DOFs.

To ensure that Eq. (1) is reversible, $\mathbf{H}_{41}^{AB\ +}$ is used to write the following equations:

$$\mathbf{X}_1 = \left(\mathbf{H}_{41}^{AB}\right)^{+}\mathbf{Y}_4 \tag{2}$$

$$\mathbf{Y}_3 = \mathbf{H}_{31}^{AB}\left(\mathbf{H}_{41}^{AB}\right)^{+}\mathbf{Y}_4 \tag{3}$$

Eq. (3) relates response of the target and indicator points to each other. Therefore, the transmissibility matrix $\mathbf{T}_{34}^{AB}$ is given by:

$$\mathbf{T}_{34}^{AB} = \mathbf{H}_{31}^{AB}\left(\mathbf{H}_{41}^{AB}\right)^{+} \tag{4}$$

$\mathbf{H}_{31}^{AB}$ and $\mathbf{H}_{41}^{AB}$ are $p \times o$ and $n \times o$ matrices. Therefore, the transmissibility matrix dimension is $p \times n$ and dependency to the excitation DOFs, o, vanishes. This means excitation forces are observable from the indicator DOFs. On the other hand, considering response of the indicator points based on the interface force and also reversibility, transmissibility matric, $\mathbf{T}_{34}$, solely within the passive subsystem is defined:

$$\mathbf{T}_{34} = \mathbf{H}_{32}^{B}\left(\mathbf{H}_{42}^{B}\right)^{+} \tag{5}$$

Fig. 1 presents the graphical concept of transmissibility.

Due to the reversibility requirements, indicator points must be carefully selected to guarantee the observability of the m coupling DOFs from n indicator DOFs.

Measuring response of the target and indicator points, $\mathbf{Y}_3$ and $\mathbf{Y}_4$ under r different independent operational conditions provides sufficiently large data sets to conduct statistical analyses for transmissibility matrix calculation. The method, known as OTPA, for all r conditions

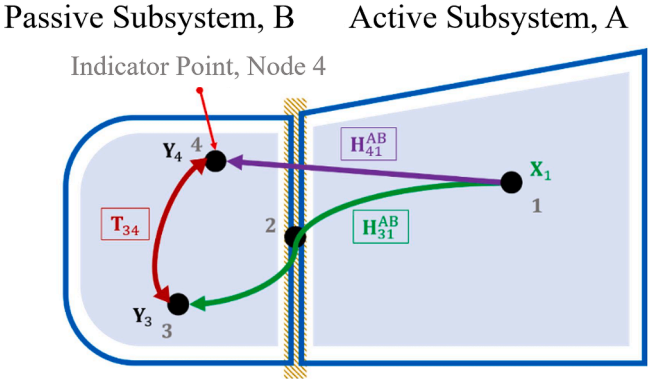

Fig. 1. Transmissibility Concept.

requires:

$$[\mathbb{Y}_3]_{p\times r} = [\mathbf{T}_{34}]_{p\times n}[\mathbb{Y}_4]_{n\times r} \tag{6}$$

where

$$[\mathbb{Y}_3] = \left[\mathbf{Y}_3^{(1)}\mathbf{Y}_3^{(2)}\cdots\mathbf{Y}_3^{(r)}\right] \tag{7}$$

$$[\mathbb{Y}_4] = \left[\mathbf{Y}_4^{(1)}\mathbf{Y}_4^{(2)}\cdots\mathbf{Y}_4^{(r)}\right] \tag{8}$$

The criterion $n \le r$ is essential to ensure the reversibility of $\mathbb{Y}_4$ (right pseudo-inverse) and Eq. (6). Hence, the indicator points must meet particular requirements: their number should be sufficiently high to avoid neglecting some paths. However, too many indicator response signals can lead to poor conditions for $\mathbb{Y}_4$, complicating inversion process and amplifies the effect of noises on the results. Therefore, the number and position of indicator points, as inputs of the method, are critical factors.

Sensitivity describes how variations in input influence the output. In the framework of transmissibility concepts, input and output are responses at the indicator and target points), respectively. In this concept, since each indicator DOF represents an independent path, sensitivity matrix components convey the sensitivity of the target DOF response signal to the path. Sorting the sensitivity components for each target DOF ranks the paths that transfer the signal according to their influence on the target signal.

Contribution analysis is a technique used to identify how much each feature contributes to predicting the target variable. In the context of TPA, it reveals the contribution of each path, which is equal to the measured transfer function multiplied by the source strength [21].

A conventional method to solve Eq. (6) and calculate the transmissibility matrix, $\mathbf{T}_{34}$, is the utilization of H estimators. The pseudo-inverse matrix of $\mathbb{Y}_4$ is

$$\mathbb{Y}_4^{+} = \left(\mathbb{Y}_4^T\mathbb{Y}_4\right)^{-1}\mathbb{Y}_4^T \tag{9}$$

Combining Eq. (9) and Eq. (6) leads to:

$$\mathbf{T}_{34} = \mathbb{Y}_4^{+}\mathbb{Y}_3 = \left(\mathbb{Y}_4^T\mathbb{Y}_4\right)^{-1}\mathbb{Y}_4^T\mathbb{Y}_3 \tag{10}$$

Definition of the averaged Auto Power Spectrum (APS) matrix of $\mathbb{Y}_4$, $G_{\mathbb{Y}_4\mathbb{Y}_4}$, and the averaged Cross Power Spectrum (CPS) matrix between $\mathbb{Y}_4$ and output signals $\mathbb{Y}_3$,$G_{\mathbb{Y}_3\mathbb{Y}_4}$ are:

$$G_{\mathbb{Y}_4\mathbb{Y}_4} = \frac{1}{r}\mathbb{Y}_4^T\mathbb{Y}_4 \tag{11}$$

$$G_{\mathbb{Y}_3\mathbb{Y}_4} = \frac{1}{r}\mathbb{Y}_4^T\mathbb{Y}_3 \tag{12}$$

Using them in Eq. (10), we have

$$\mathbf{T}_{34} = G_{\mathbb{Y}_4\mathbb{Y}_4}^{-1}G_{\mathbb{Y}_3\mathbb{Y}_4} \tag{13}$$

This presents the transmissibility matrix based on the H_1 estimator of APS and CPS of the measured DOFs. The H_1 estimator uses the average APS to increase the rank and ensure invertibility.

Other methods to calculate pseudo inverse matrix of $\mathbb{Y}_4$ includes decomposition methods such as SVD. However, difficulties arising from the inversion of $G_{\mathbb{Y}_3\mathbb{Y}_4}$ may complicate the estimation of the transmissibility matrix; for instance, noise amplification caused by the $G_{\mathbb{Y}_3\mathbb{Y}_4}$ poor condition or rank deficiency of $G_{\mathbb{Y}_3\mathbb{Y}_4}$.

Despite the potential advantages of OTPA method, there are some limitations to its practical implementation. Here, we mention the main challenges and some considerations necessary to address them:

1- **Mathematical difficulties:** according to Eq. (10), the existence of $\mathbb{Y}_4^{+}$ needs $n \le r$. In other words, the number of independent excited load cases must exceed the number of indicator DOFs. Reference [22]

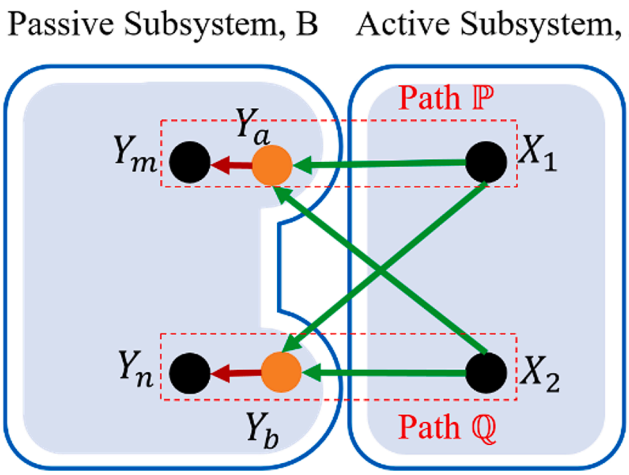

Fig. 2. Cross-Coupling in OTPA Methods.

has compared the results of TPA and OTPA methods for a vehicle. At each frequency, the number of present orders represents the independent load cases. According to the findings, to obtain reliable results from the OTPA method, the number of orders should at least be twice the number of paths (indicator points). As the number of load cases increases, the errors of the OTPA method, compared to classical TPA decreases.

On the other hand, since correlated indicator signals carry similar information, coherence between signals measured at indicator points lead to reduced independence. This causes rank deficiency and estimation error.

2- **Cross-coupling effect:** The dynamic system presented in Fig. 2 includes two paths between the active and passive subsystems. These paths transfer excitation signals X_1 and X_2 to target points m and n to produce the response signals Y_m and Y_n.

In addition to the sources on the excited paths, other sources also affect the response signal. This phenomenon is the cross-coupling effect, is displayed in Fig. 2. Therefore, the signals at target points are:

$$Y_m = H_{m1}X_1 + H_{m2}X_2 \tag{14}$$

$$Y_n = H_{n2}X_1 + H_{n2}X_2$$

3- **Effect of neglected path:** Paths considered in a TPA are independent, meaning that neglecting some of them does not invalidate the estimation of others' contributions. However, in OTPA, depending on the degree of correlation between the neglected path and others, the entire contribution analysis can become inaccurate and unreliable. The more correlated the neglected path is to others, the more severe the errors it causes in the partial contribution of those paths.

4- **Evaluation difficulties:** A standard method for evaluating a TPA process is to compare the measured target signal to the synthetized one from the path contributions. An insignificant difference indicates reliable results. However, OTPA is based on a backward-forward calculation process that distributes the measured response signal between the considered paths. As a result, some contributions will be assigned to the considered paths, which masks the effect of neglected paths or the redundant paths in the synthetized signal.

Overall, the most qualified OTPA requires low coherence between excited load cases, minimal cross-coupling between the indicator signals and inclusion of all significant path in the analysis.

The proposed method utilizes the advantages of ML to address mathematical difficulties. In addition to its ability to handle large data sets, provided by more independent excited load cases and a greater number of indicator DOFs, the ML approach eliminated the need for matrix inversion. A common approach to deal with singularity in matrix inversion is truncation of singular values bellow a specific threshold. Threshold determination plays a crucial role in the accuracy of the final results. However, even the optimal threshold causes some extent of information loss. Depending on the nature of the case, lost information may cause inaccurate results and misjudgement about the most problematic paths for noise/ vibration transfer. Thus, the ML-OTPA lead to more comprehensive and accurate investigation. However, three other limitations of classic OTPA are its inherent issues.

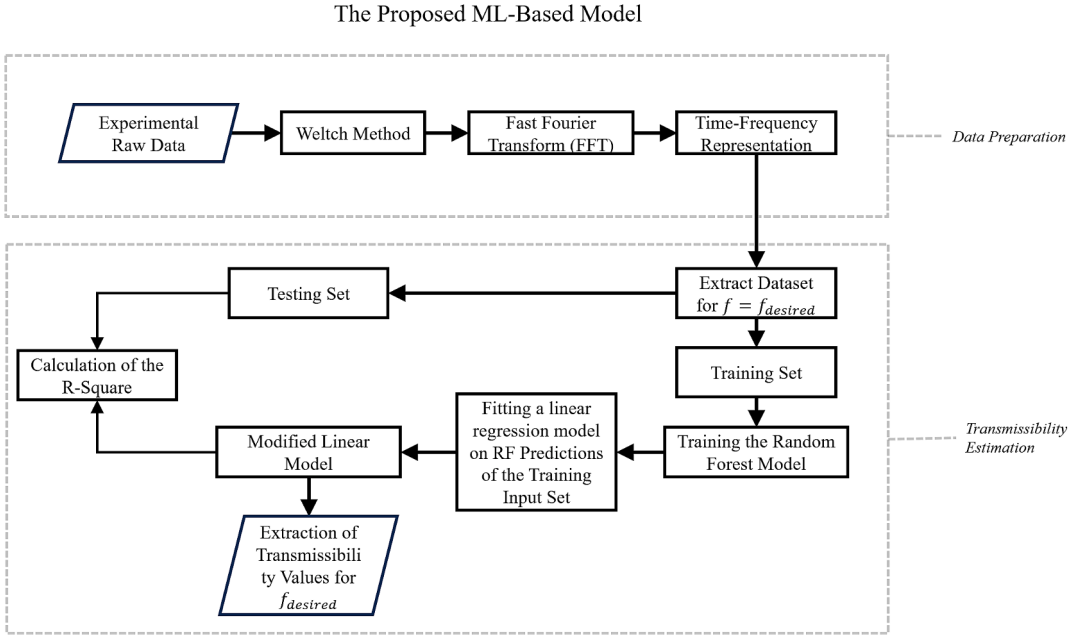

Fig. 3. Flowchart of the proposed method for data preparation and transmissibility function estimation using a hybrid random forest algorithm and linear regression approach.

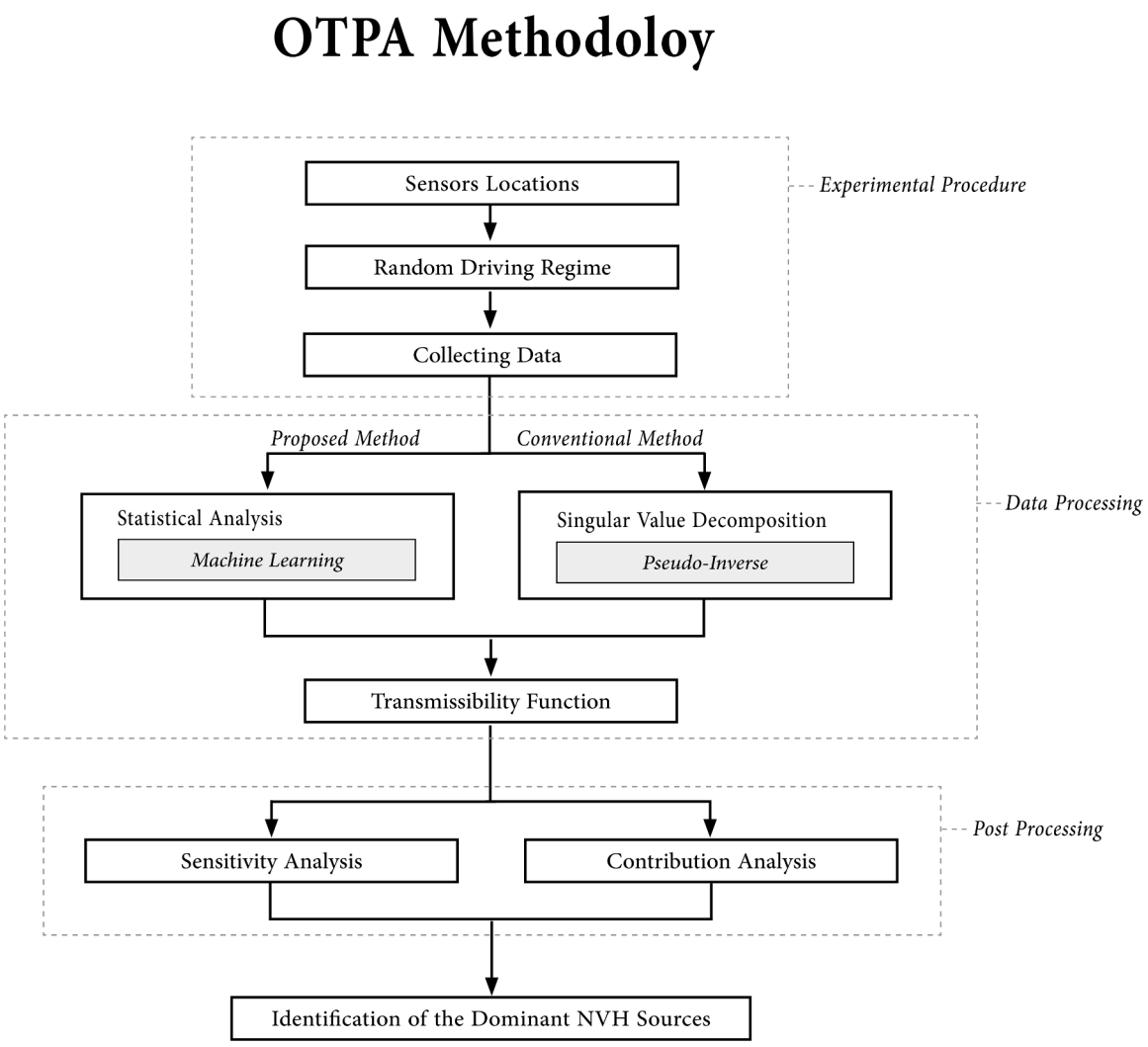

Fig. 4. ML-enhanced OTPA method.

3. Machine learning-based OTPA

Applying matrix inversion for OTPA presents several challenges, including computational complexity and sensitivity to noise in operational data. ML approaches have the potential to address these difficulties by efficiently handling large datasets, identifying complex patterns, and generating reliable predictions. Moreover, with sufficient data collected under various driving conditions, these algorithms can deliver more reliable and accurate predictions, ultimately improving the overall performance of OTPA.

To solve the OTPA problem, regression algorithms are employed. The present study utilises the Random Forest (RF) algorithm to manage multiple channels and complex data structures. In addition to the mentioned advantages, the RF framework's feature importance analysis offers valuable insights into the contributions of individual features, aiding in optimal decision-making for the identification of NVH sources. Section 3.1 outlines the specifications of RF algorithm, while Section 3.2 demonstrates its implementation within our OTPA methodology.

3.1. Estimation of transmissibility functions using the proposed ML-based approach

RF is an ensemble ML technique based on the concept of bagging, or bootstrap aggregation. Bagging is a method used to reduce the variance of an estimated prediction function, and it is particularly effective for high-variance, low-bias procedures such as decision trees. The advantage of utilizing RF in solving OTPA equations lies in its ability to preserve essential information in the indicator matrix. This contrasts with the conventional method (SVD), which imposes modifications on the matrix to make it suitable for inversion. Another benefit of this approach is its consideration of the inherent nonlinearities in the developed relationship (model) between the indicator sensor values (inputs) and the target Sound Pressure Level (SPL) or acceleration (output). In this section, a novel hybrid method combining RF and linear regression is introduced (as it is described in Fig. 3) for the high-precision solving of the OTPA equations.

Preparation of the input data involves using the welch method for

Table 1
Tested vehicle specification.

Vehicle category	M1
Body variant v	Compact sedan
Kerb mass	1390 Kg
Engine	1.5 L straight-four engine M15TC/2027378 with turbocharger
Front Suspension	MacPherson strut
Rear Suspension	Coupled Torsion Beam (Twist-Beam)
Tires	Type P, width 185 mm, aspect ratio 65 %, diameter 17-inch, load index 560 kg, speed rating 210 km/h (88H)

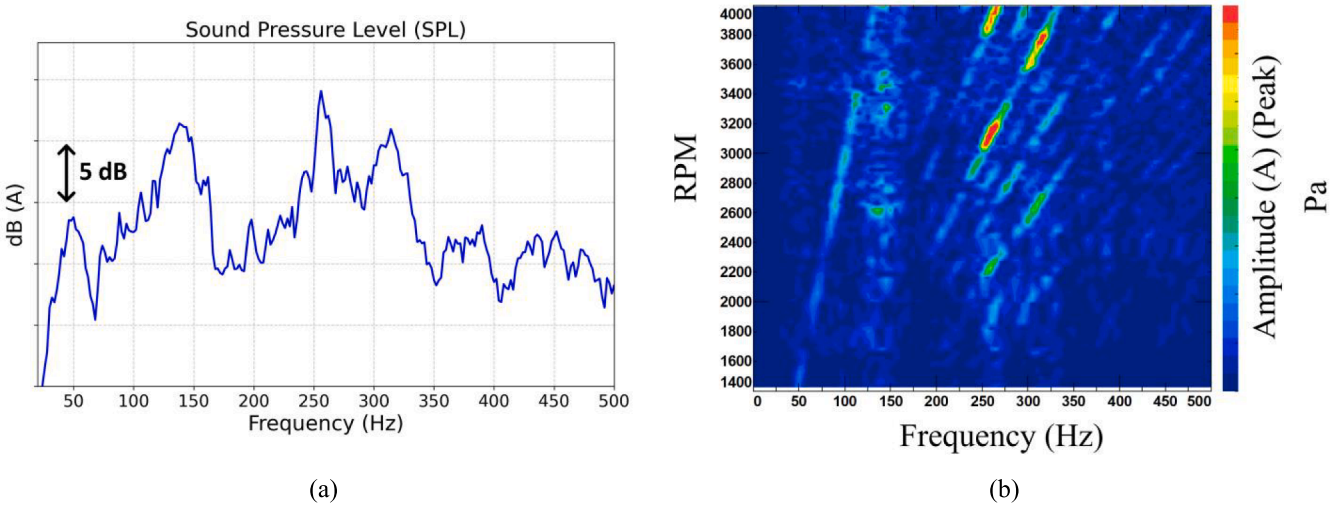

Fig. 5. Interior noise analysis during run-up test: (a) SPL profile; (b) Frequency domain response.

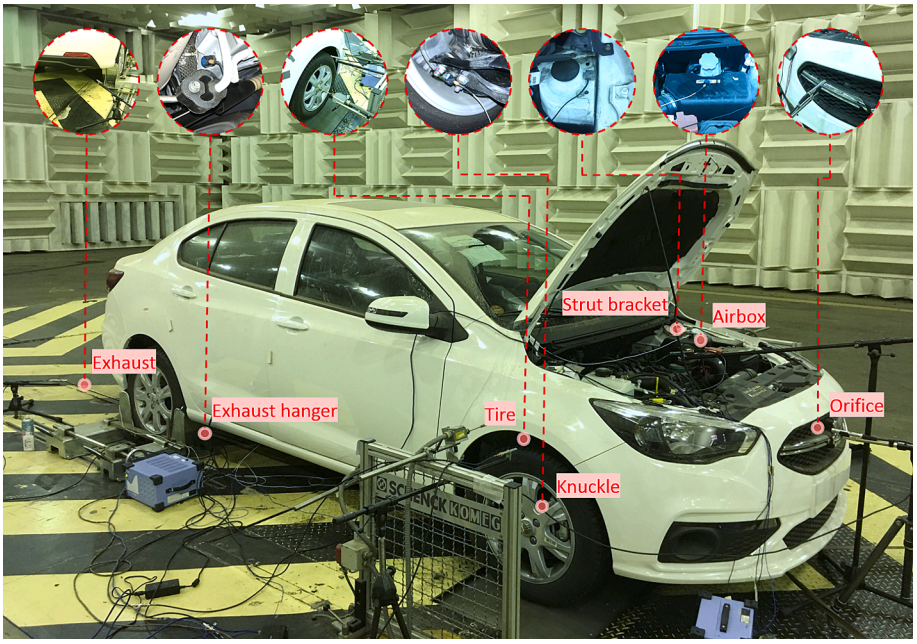

Fig. 6. Actual Indoor Random Test Setup in NVH Laboratory.

Table 2
Used equipment specification.

Name	Type	Frequency range [Hz]	Specification
Microphone	4188	8–12.5 k	½-inch free-field mic, pre-polarized
Accelerometer	356A11	1–5 k	Sensitivity: (±10 %)10 mV/g (1.02 mV/(m/s^2)), Measurement Range: ±500 g pk (±4900 m/s^2 pk)
Signal Analyzer	SA-02 M	to 40 kHz	Up to 24 channels

discretizing the time data recorded in RPM variable tests into short-time segments. The data recorded in each of the time segments will be introduced as a separate dataset into the model. Fast Fourier Transform (FFT) is applied on each of the segments to obtain the time–frequency representation of the recorded signals. Consequently, each dataset is represented as an $m \times n \times r$, where m refers to the aggregated number of time segments in all of the performed tests; n refers to the number of indicator sensors and r refers to the number of frequencies which are obtained using FFT.

The RF model is trained using bootstrap aggregation to capture the relationship between the values of the indicator sensors and the target sensor. The general steps involved in constructing a RF model are as

(a) (b) (c)

Fig. 7. Test equipment (a) Accelerator (PCB piezotronics), (b) Microphone (Brüel & Kjaer), (c) Signal analyzer (RION).

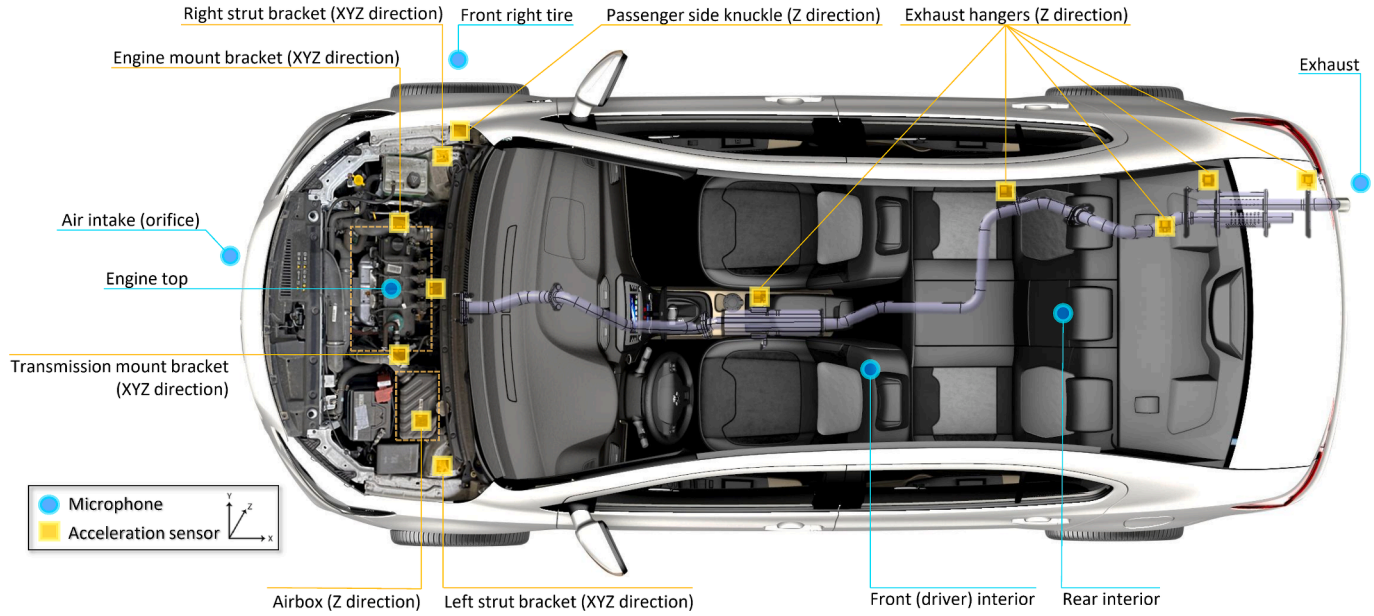

Fig. 8. Microphones and accelerometers position on the vehicle.

follows [23]:

1. A bootstrap sample is drawn from the training data for each tree. At each node, a random subset of m variables are chosen as potential candidates for splitting.
2. Each tree is grown to its full depth without pruning, allowing it to generate its prediction.
3. The final prediction is obtained by averaging of the predictions made by all the trees.

Although the RF model generates predictions for the target sensor value based on the indicator sensor values, it does not provide explicit linear coefficients (referred to as transmissibility in this context). To derive the transmissibility values, linear regression is applied to the trained RF model in the next step.

The R-Square metric was employed to evaluate the performance of the ML-OTPA and SVD methodologies by comparing their predicted SPL at the driver's ear microphone with the experimentally measured values. The R-Square value was calculated using the formula [24]:

$$R^2 = 1 - \frac{\sum \left(Y_{exp} - Y_{pred}\right)^2}{\sum \left(Y_{exp} - \overline{Y}_{exp}\right)^2} \tag{15}$$

where Y_{exp} represents the experimentally recorded SPL at the driver's ear microphone, Y_{pred} is the SPL predicted by the respective method (ML-OTPA or conventional OTPA), and $\overline{Y}_{exp}$ is the mean of the experimental values.

3.2. Utilization of machine learning in OTPA method

Fig. 4 provides an overview of the OTPA methodology, comparing the conventional method with the proposed ML approach, ML-OTPA. The figure illustrates how both methods follow the same approach in terms of test setup and post-processing but differ in their data processing techniques. The conventional OTPA employs truncated SVD to reduce the dimensionality of the indicator matrix. While effective, this approach is subject to inherent limitations. The accuracy of the final transmissibility function may be compromised by the artificial

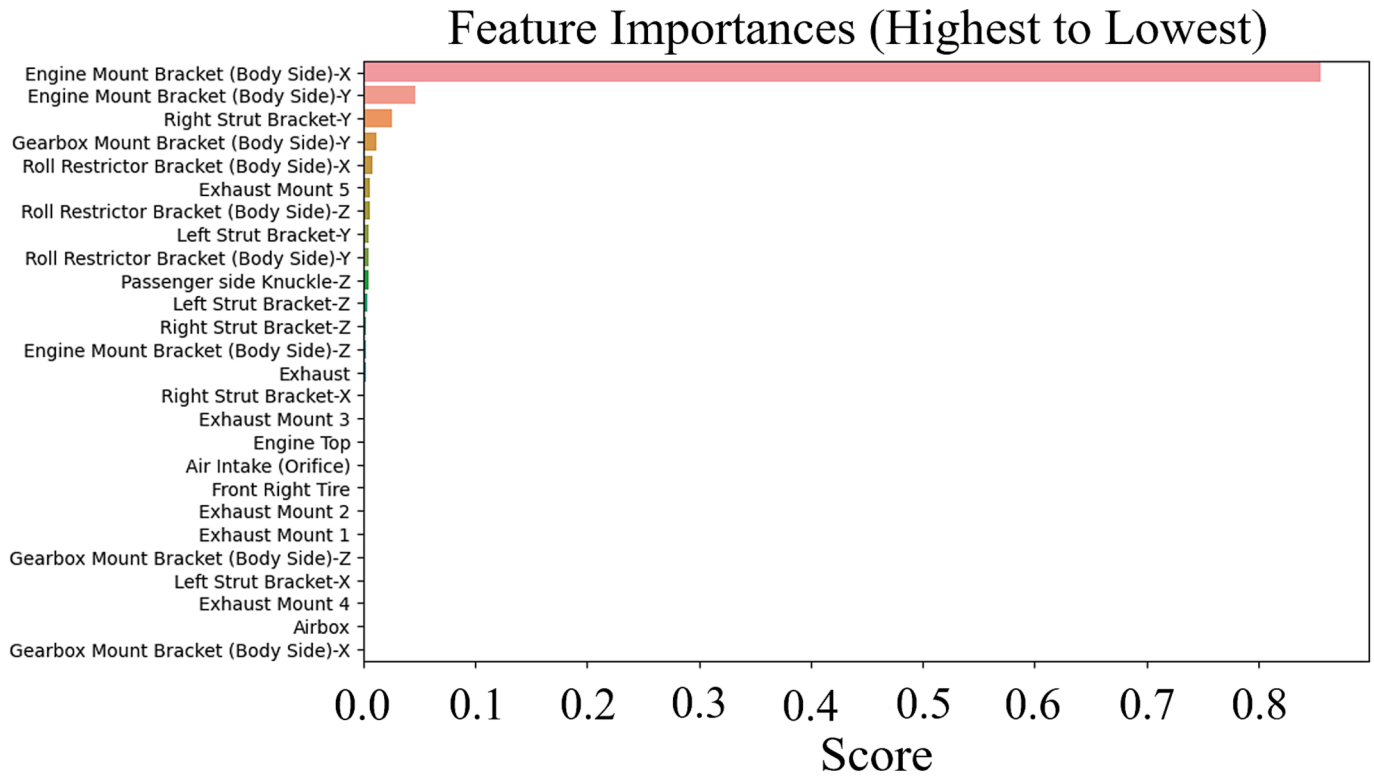

Fig. 9. Feature importance analysis.

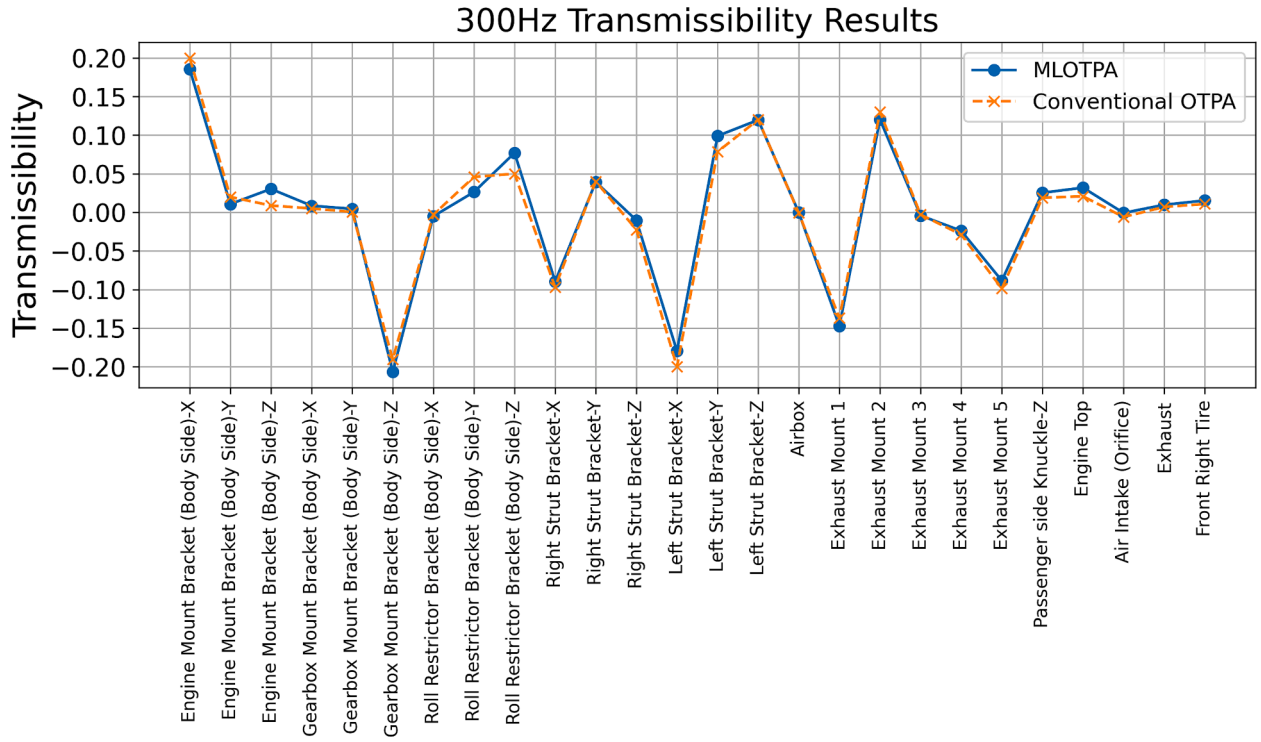

Fig. 10. Comparison of transmissibility for conventional OTPA and ML-OTPA method.

modifications introduced through SVD. Furthermore, the reduction of singular values may result in information loss, especially in intricate systems such as vehicles, where precise transmissibility estimates are essential for accurately identifying NVH sources.

To overcome these limitations, the proposed ML-driven OTPA method (ML-OTPA) eliminates the need for such mathematical adjustments. Instead of relying on SVD to analyse the indicator matrix, ML is used to directly establish the correlation between operational inputs and

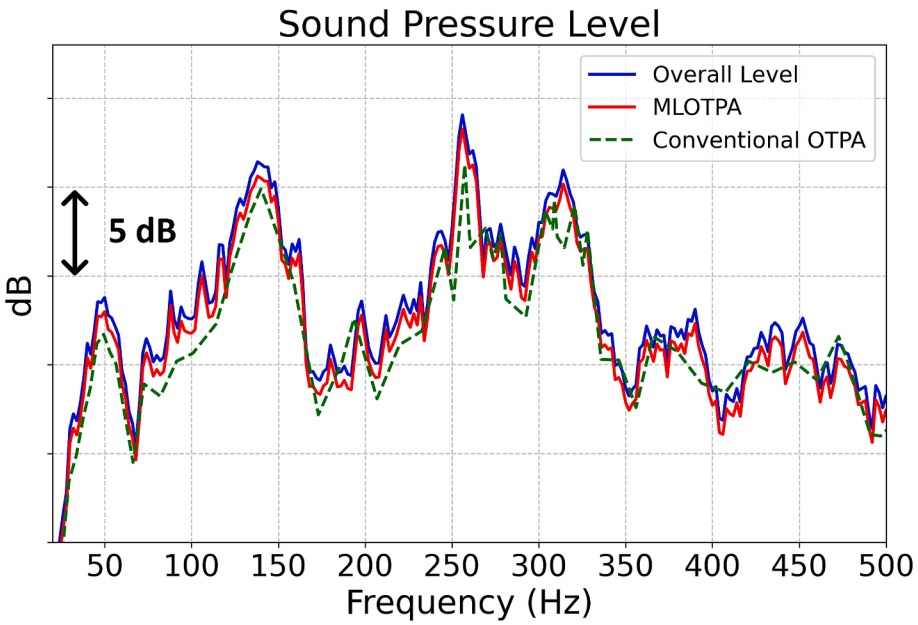

Fig. 11. Measured SPL signal vs. synthesized signals from ML-OTPA and conventional OTPA models.

Table 3
Performance comparison of ML-OTPA and conventional OTPA in different operational conditions.

Operational Condition	Accuracy (%)	
	ML-OTPA	**Conventional OTPA**
Runup – G1	98.5	93.7
Run down – G1	98.2	92.8
Runup – G2	98.8	94.5
Run down – G2	97.7	93.4
Runup – G3	98.7	93.3
Run down – G3	98.3	91.6
Runup – G4	97.8	94.4
Run down – G4	98.4	92.6
Runup – G5	96.7	93.2
Run down – G5	97.5	91.7
Standstill	98	94.3

responses, based on the system's underlying physics. By analysing experimental data, the ML model develops an intrinsic understanding of transmissibility without restoring to dimensionality reduction methods.

Moreover, this approach enables more flexible data management, accommodating complex systems with numerous input and output channels- an area conventional OTPA methods often encounter difficulties. The ML model is capable of identifying non-linearities and intricate relationships in the data, which conventional linear methods such as SVD may fail to capture effectively.

4. Application in automotive industry

4.1. Case study

Automotive industry products are typically systems composed of components with various dynamic profiles. In a typical fuel-powered car, the engine is the primary source of excitation and acts as the active subsystem, while other parts, such as the car body, are considered as passive subsystems. This distinction between components based on their dynamic properties has driven the use of TPA to study, investigate, and optimize the vibro-acoustic behaviour of vehicles. Previous studies in this field have reported the use of classical TPA [5,25,26] and OTPA [11,13] methods to identify contributions of different paths in transmitting noise and vibration throughout a vehicle.

Given the nature of a car system, which aligns with the requirements of OTPA, and the extensive literature available on this subject, this study presents the application and results of the proposed method for a passenger car. The specifications of the vehicle used are summarized in Table 1.

An interior noise analysis for the vehicle was conducted during a run-up test. The SPL of the interior noise, recorded at the driver's right ear position using a microphone, is shown in Fig. 5(a). Additionally, Fig. 5 (b) presents interior noise in the frequency domain during the rapid acceleration. High levels of noise or vibration at specific frequencies, independent of engine speed, appear as vertical lines in spectrograms where frequency is plotted on the horizontal axis, indicating the occurrence of resonance. The prominent vertical region with elevated noise levels in the frequency range of 250–350 Hz indicates the presence of resonances.

4.2. Test setup

4.2.1. Laboratory, equipment, and vehicle specification

To evaluate the noise and vibration characteristics of the vehicle under various operating conditions, indoor random driving tests were conducted in hemi-anechoic chamber equipped with a single axle chassis dynamometer. The tests were conducted at an average ambient temperature ranging from 28 to 30 °C, an average humidity of 16 to 18 %, a wind speed of 2.1 to 2.6 m/s, and a background noise level of 50 dB. Fig. 6 shows an actual indoor random test setup which were performed at vehicle level in NVH laboratory.

Specifications and images of measuring equipment utilized in this study are presented in Table 2 and illustrated in Fig. 7, respectively.

4.2.2. Sensor positioning and test procedure

Accurately interpret OTPA results is impossible without a comprehensive understanding of sound and vibration propagation, as well as

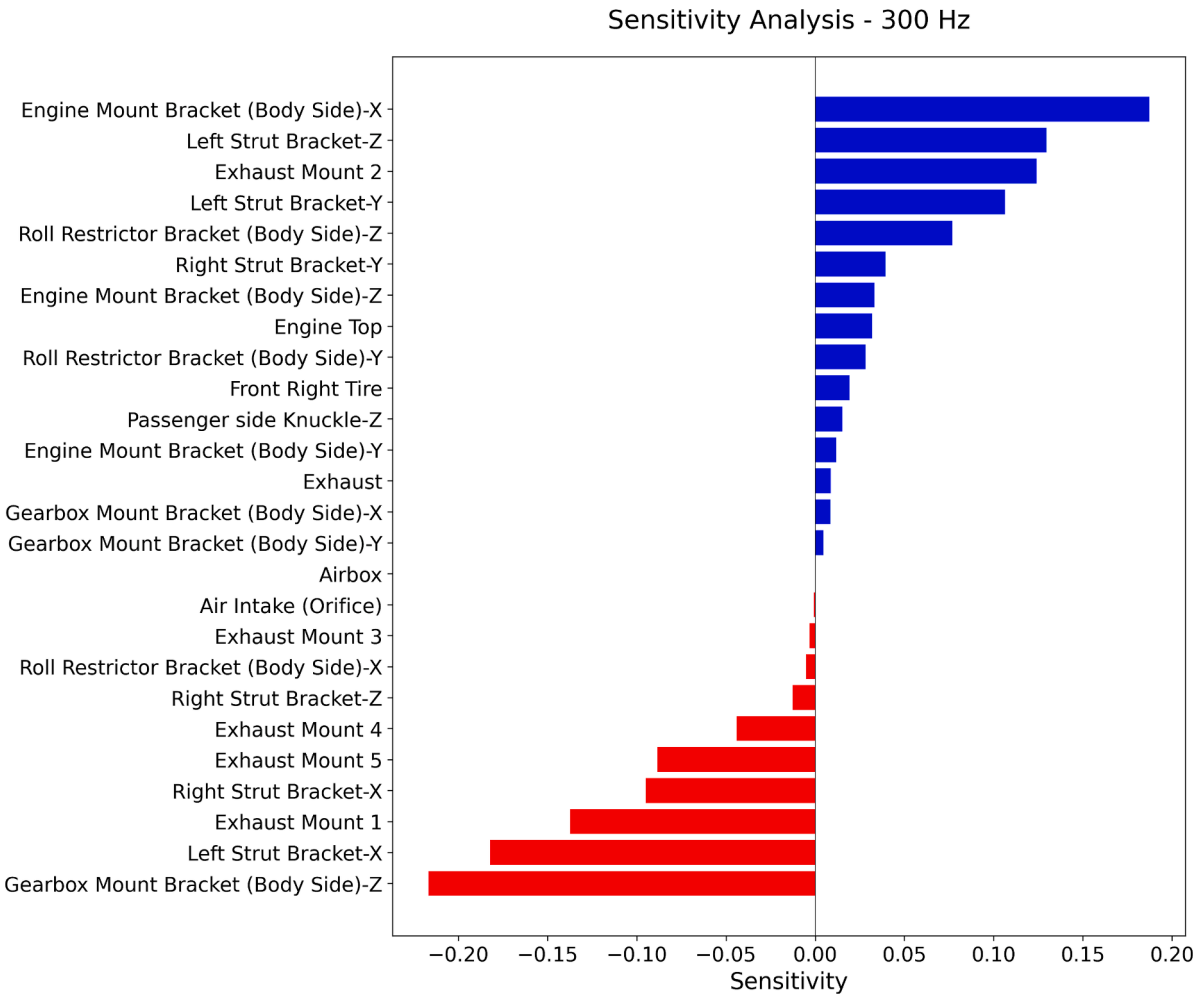

Fig. 12. Sensitivity analysis at 300 Hz.

sensor positioning, both of which are essential for identifying sources and receivers. The placement and number of target and indicator response sensors were carefully selected to prevent noise amplification during inversion and to avoid path neglect and inaccurate contribution estimation. During the test, a multi-channel signal analyzer was used to collect a total of 28 reference signals, including six sound signals and 22 vibration signals captured from microphones and accelerometers, respectively. Interior noise data were collected using two receiver microphones mounted inside the vehicle in accordance to BS ISO 5128:2023 [27]. Exterior microphones were installed in position near possible sources including air intake (orifice), front right tire, exhaust, and top of engine. In addition, three-axis indicator accelerometer sensors were attached to engine mount bracket, gear mount bracket, roll restrictor bracket, and right/left struct brackets, also one-axis accelerometers were installed in airbox and five exhaust mounts. The location of sound pressure sensors and acceleration sensors are shown in Fig. 8.

To obtain reliable OTPA results, measurements should be conducted under a range of operating conditions, including variations in engine torque, speed, gear, and RPM. Accordingly, tests were run under different typical operating conditions, such as standstill (idle), engine run-ups (acceleration) with half and wide-open throttle across all five gears of the vehicle, steady speed, and coast down (deceleration). Each data acquisition session lasted approximately 20 s. For instance, during a runup in 3rd gear, starting from an engine speed of 1500 RPM, accelerator pedal was pressed almost fully (wide-open throttle) until reaching the highest possible engine speed for that gear was reached. The resulting sound pressure levels and vibrations were measured, with the test repeated for three times. In accordance with the study's objective of capturing the car's dominant frequency range of noises up to 8 kHz, all signals were meticulously measured at a sampling frequency of 25.4 kHz. To optimize data processing, an averaging time block of 0.5 s (equivalent to 16,384 samples, a power-of-two integer) was employed.16,384 samples include samples recorded in 0.5 s and 3864 padded zeros help to ensure increasing accuracy of FFT. Analyzing the recorded signals at discrete time steps produces low-coherence inputs, serving as independent operational conditions.

4.3. Results

This section presents the application of the proposed method for

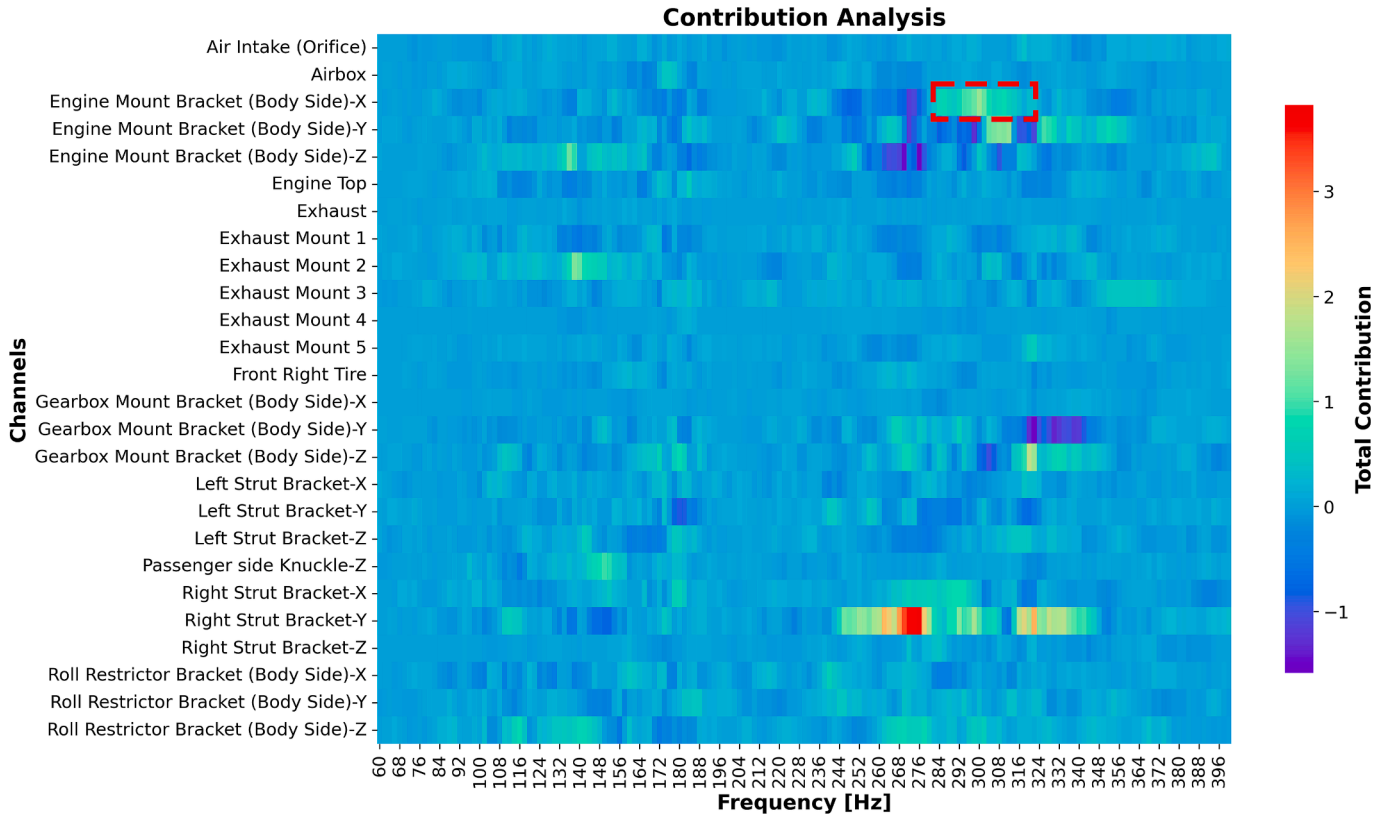

Fig. 13. Contribution analysis.

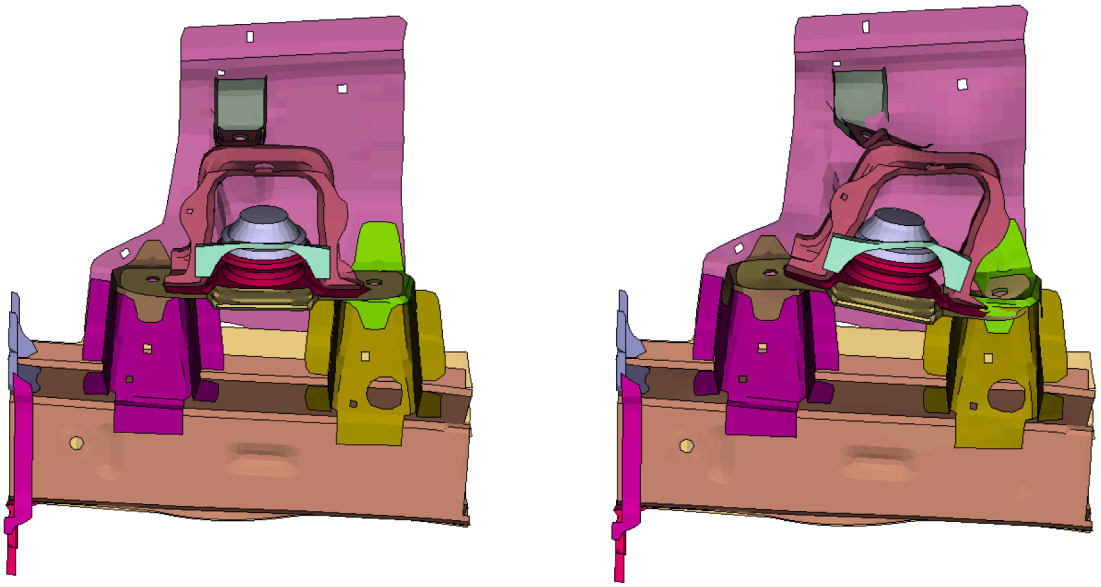

(a) (b)

Fig. 14. The mode shape corresponding to 300 Hz natural mode of the engine mounting bracket: (A) Normal Shape (B) Deformed shape.

conducting various analyses, including feature importance, sensitivity analysis, and contribution analysis. The final findings from the real case study, along with an assessment of the effectiveness of modifications inspired by the ML-OTPA test to enhance the NVH profile of the system, are used to evaluate the method's performance. A comparison of the R-squared errors for the proposed method and SVD confirms its reliability and accuracy.

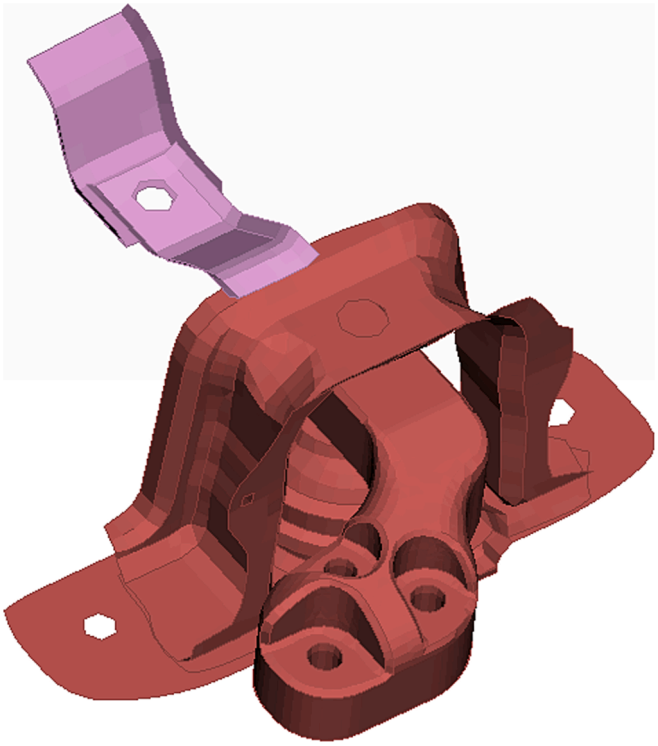

Fig. 15. The lateral connection arm of the engine mounting bracket.

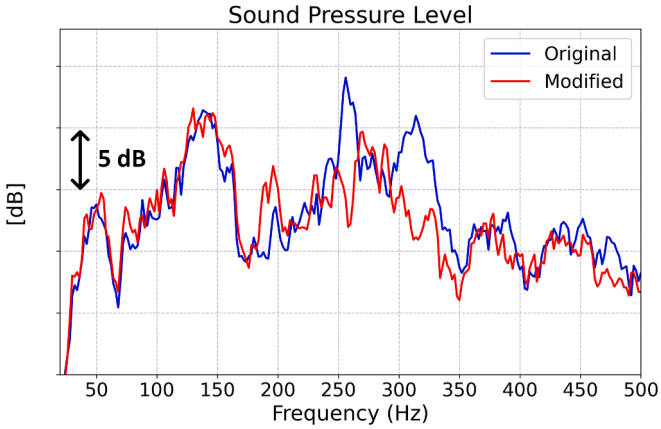

Fig. 16. SPL improvements.

4.3.1. Learning evaluation

Random Forest Regression (RFR) from the scikit-learn library was used to construct the model, with a training size of 70 %, a test size of 30 %, and a random state of 42. The total computational time required for training the RFR model across the entire frequency range was approximately 574 s, executed on a system with an Intel Core i7 processor and 32 GB of RAM. The training was performed for frequencies ranging from 10 Hz to 500 Hz in 5 Hz intervals, resulting in a total of 99 frequency steps. On average, the training time for each individual frequency point was approximately 5.8 s, leading to the total duration of $5.8 \times 99 \approx 574$ s. The model achieved an R-squared accuracy of 0.986. Feature importance was analyzed solely at 300 Hz, the critical NVH-related frequency. The results, illustrated in Fig. 9, indicate that the engine mount bracket in the x-direction exhibits the strongest relationship and the greatest impact on the target channel, confirming its dominant contribution to the interior noise problem at this frequency.

To evaluate ML-OTPA and conventional OTPA at 300 Hz, predicted SPL values were compared to experimentally recorded SPL at the driver's ear. This comparison yielded R-squared accuracy scores: 97 % for ML-OTPA and 93 % for conventional OTPA, demonstrating a notable advantage for the ML approach. Subsequently, these two methods were used to calculate transmissibility, which is illustrated in Fig. 10. The superior R-squared accuracy of ML-OTPA directly translates to more accurate transmissibility estimations, crucial for effective NVH source localization and assessment.

Fig. 11 displays the SPL results predicted by both the conventional OTPA and the proposed ML-OTPA method. Both models were created using 70 % of the data for training and 30 % for testing. The ML-OTPA predictions correspond more accurately with the overall level derived from the experimental data. This shows that ML-OTPA is more accurate in producing the target signal than the conventional OTPA method.

Table 3 also offers a comparison of the accuracy of both methods under various operational conditions. The results clearly indicate that ML-OTPA consistently achieves higher accuracy than the conventional OTPA method.

4.3.2. Sensitivity analysis

For further analysis, the selected frequency of 300 Hz is shown in Fig. 12. The "engine mount bracket" exhibits the highest positive phase value in the x-direction, while the "gearbox mount bracket" demonstrates the most considerable negative phase value in the z-direction.

4.3.3. Contribution analysis

The contribution analysis was performed to measure the impact of different noise paths on the target channel within the vehicle's interior noise. The suggested method, which calculates the transmissibility matrix, split the operational data into distinct partial contributions, providing the impact of each path. The data presented in Fig. 13 illustrate the comparative contributions of various noise paths, notably indicating that the engine mount bracket-X significantly impacts internal noise at about 300 Hz.

Based on the assessments of feature importance, sensitivity, and contribution analysis, the engine mount bracket in the x-direction was identified as the primary cause of the interior noise issue, particularly at 300 Hz. To validate this findings, additional analyses were conducted to ensure the accuracy and reliability of the ML-OTPA approach. Following these analyses, modifications were implemented to address the identified noise sources, and interior noise tests were conducted to assess the effectiveness of these changes.

4.3.4. Detection of excessive vibration causes

As a result of the OTPA, the right-hand engine mount in the longitudinal (X) direction was identified as the most significant contributor to the driver's ear SPL. However, this knowledge alone is insufficient to improve the SPL at the desired position. The next essential step is to identify the cause of the excessive vibration in this path, particularly at a frequency of 300 Hz, to achieve the desired improvement.

A highly effective approach for identifying the cause of excessive vibration at a narrow-band frequency is modal analysis. Modal analysis can reveal the potential resonance frequencies of a system, along with the mode shapes and damping values corresponding to each natural frequency. Therefore, a modal analysis was performed on the entire vehicle to determine if there is a natural mode that plays a crucial role in the excessive vibration passing through the right-hand engine mount

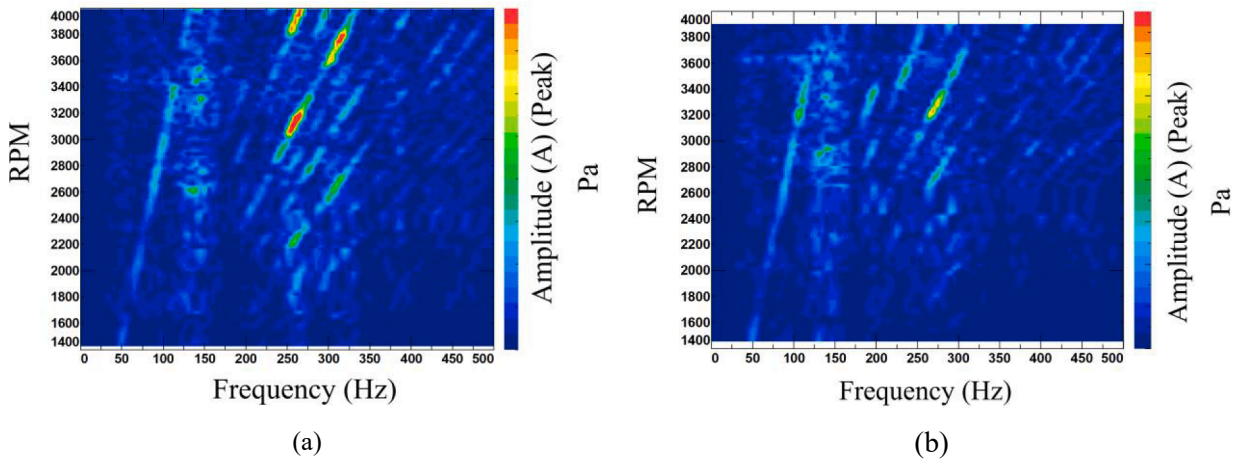

Fig. 17. Frequency domain response comparison (a) Before and (b) After modifications.

path to the driver's ear. The experimental modal analysis revealed a local natural mode with a frequency of 300 Hz on the bracket that connects the right-hand engine mount to the body in the lateral direction (as depicted in Fig. 14). As a result of this natural mode, the harmonic force applied by the engine to the right-hand engine mount leads to peak in acceleration (resonance), which is transferred to other parts of the automotive body, as well as to the panels surrounding the passenger cabin, such as the roof, floor, and firewall; This causes these panels to generate boom noise, potentially at 4500 RPM, 3600 RPM, 3000 RPM, 2571 RPM, and 2250 RPM, which correspond to the 4th, 5th, 6th, 7th, and 8th engine orders, respectively.

The dynamic weakness of the right-side engine mount bracket, or its mounting location on the Body in White (BIW), is the main cause of resonance at 300 Hz. According to the above explanations, there are three solutions to this problem. As the best solution, we decided to remove the lateral connection of the engine mount bracket (as it is shown in Fig. 15). This connection was identified as the most significant path contributing to interior noise at 300 Hz, based on the OTPA and modal analysis results. This is an ideal solution due to its low manufacturing cost, weight reduction, and accelerated assembly.

4.3.5. Improvement based on ML-OTPA results

Fig. 16 illustrates the modifications made to the vehicle and compares the before-and-after SPL results, showing an improvement of 2.2843 %. Fig. 17 displays the RPM-frequency map (spectrogram) of the interior SPL before (a) and after (b) the changes. The changes clearly address the problematic frequency range, which was identified as the primary source of the noise issue.

5. Conclusion

In the present work, a ML-based TPA method, ML-OTPA, was proposed based on RFR, which offers advantages over conventional OTPA approaches. It was demonstrated that selection of the most crucial resonant frequencies in the target noise or vibration is the essential step that should performed prior to the OTPA test. For this purpose, an interior noise analysis of the vehicle was conducted during a run-up test. The frequency domain SPL of the interior noise revealed 300 Hz as the most critical resonant frequency, which should be selected for the OTPA analysis. According to the findings the R-square metrics for the proposed and SVD methods are 97 % and 93 %, respectively. The OTPA analysis led the right-side engine mount (X-direction) to be the most contributing path in the driver's ear noise. Since both sensitivity and contribution values are relatively high in this path, the transmissibility of the mounting location of this engine mount to the driver ear's location is the root of dominance.

On the other hand, the modal analysis on this area revealed that the lateral connection of the engine mount to the BIW has a natural mode shape in this frequency. As an improving solution, we decided to remove the weak path (the lateral arm of the right-side engine mount) and let the vibration transfer through the two other bolts on the front rail. This modification led to remarkable improvement (up to 4 dB) on the interior noise and disappearance of the 300 Hz resonance. This is a highly effective way of improvement due to its simplicity of manufacturing, assembly time reduction, and weight reduction. In conclusion, the remarkable improvement in the interior noise verified performance of the proposed method as a reliable and robust way of finding the dominant noise transfer path in a vehicle.

CRediT authorship contribution statement

Sharif Khakshournia: Writing – original draft, Validation, Software, Project administration, Methodology, Investigation, Formal analysis, Conceptualization. **Shaygan Shahed Haghighi:** Writing – original draft, Software, Methodology, Investigation, Formal analysis, Conceptualization. **Marzie Majidi:** Writing – original draft, Validation, Software, Methodology, Formal analysis, Conceptualization. **Farhad Najafnia:** Writing – original draft, Software, Methodology, Formal analysis, Conceptualization. **Hamed Haddad Khodaparast:** Writing – review & editing.

Declaration of competing interest

The authors declare that they have no known competing financial interests or personal relationships that could have appeared to influence the work reported in this paper.

Appendix

A. Mathematical formulation of the random forest regression

Fig. A1 provides an overview of the entire process, highlighting the key steps of bootstrap sampling, tree construction, and predictions aggregation.

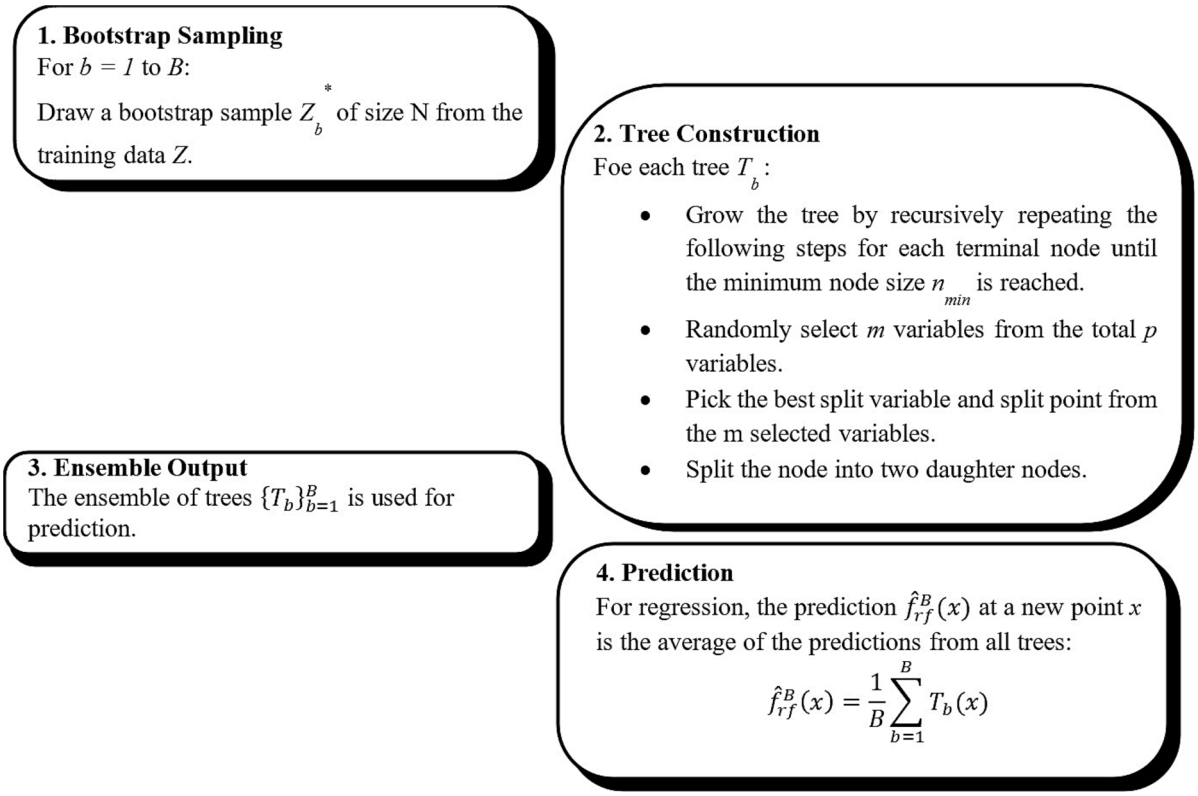

Fig. A1. Overview of the mathematical formulation for RFR [1].

Each of the variables in the diagram is defined as follows:

- b: Index of the individual tree or bootstrap sample in the ensemble, ranging from 1 to B.
- B: Total number of trees in the forest.
- Z_b^*: A bootstrap sample, created by randomly sampling (with replacement) N data points from the training dataset Z.
- Z: The original training dataset containing all data points.
- N: The size of the bootstrap sample, typically equal to the size of the original dataset Z.
- T_b: The b^{-th} decision tree constructed during the process.
- n_{min}: The minimum number of data points required in a node for it to be split further.
- m: The number of randomly selected variables (features) from the total p variables considered for splitting at each node.
- p: Total number of variables (features) in the dataset.
- $\{T_b\}_{b=1}^B$: The collection of all B decision trees in the ensemble used for prediction.
- $\hat{f}_{rf}^B(x)$: The RFR prediction at a new input point x.
- x: A new data point where the prediction is being made.
- $T_b(x)$: The prediction made by the b^{-th} decision tree for the data point x.
- $\frac{1}{B}\sum_{b=1}^{B} T_b(x)$: The average of the predictions from all B trees, which forms the final Random Forest prediction for regression.

The accuracy of a RFR model can be assessed using the Mean Squared Error (MSE) metric based on Eq. (1) [2].

$$OOB\_MSE = \frac{1}{n}\sum_{i=1}^{n}\left(y_i - \widehat{y_{iOBB}}\right)^2 \tag{1}$$

Where:

- n is the total number of observations in the dataset.
- y_i is the actual observed value of the response variable for the ith observation.
- y_{iOBB} is the average prediction for the i^{th} observation from all trees in the random forest for which this observation has been “out-of-bag” (OOB), meaning it was not used for building that particular tree.

- For each tree in the random forest, approximately one-third of the observations are left out or "out-of-bag" (OOB) during the construction of that tree. These OOB samples are used to evaluate the performance of the tree.

The OOB-MSE calculates the average squared difference between the actual observed response values and the predicted values from the trees where that observation was held out and not used for training. This provides an internal estimate of the predictive accuracy of the random forest model on unseen data. A lower OOB-MSE indicates better predictive performance of the model.

The RF algorithm provides a metric called "permutation-based MSE reduction" to assess the importance of each predictor variable. The formula for calculating this metric for a given variable X_j is:

$$OOB\_MSE_t(X_j permuted) = \frac{1}{n_{OOB,t}} \sum_{\substack{i=1 \\ i \in OOB_t}}^{n} \left(y_i - \overline{\widehat{y}_{i,t}}(X_j permuted)\right)^2 \tag{2}$$

Where:

- $n_{OOB,t}$ is the number of out-of-bag observations for tree t,
- y_i is the actual response value for observation i,
- $\overline{\widehat{y}_{i,t}}(X_j permuted)$ is the prediction from tree t for observation i after randomly permuting the values of variable X_j in the out-of-bag samples.

The permutation breaks the association between X_j and the response variable. The difference between OOB_MSE ($X_j permuted$) and the original OOB_MSE (without permuting X_j) gives the increase in MSE due to not using the correct values of X_j Averaging this difference across all trees provides the overall "variable importance" score for X_j – a higher score indicates X_j is more important for predicting the response accurately.

The basic idea behind this approach is that if a predictor variable is important for predicting the response, permuting its values should significantly increase the prediction error. Conversely, if a variable is not important, permuting its values should have little effect on the prediction error.

B. Experimental procedure and data acquisition methodology

The experimental technique was developed to acquire complete data across multiple operating situations to assure the reliability and accuracy of later analysis. Each test was selected intentionally to encompass a broad spectrum of events and minimize possible causes of mistake. Runup tests were performed to collect all critical data under typical operating settings, documenting the system's dynamic behaviour as it progresses through various speeds. Coast down experiments were incorporated to reduce the impact of engine noise and other external variables, facilitating a more precise investigation of vibration behaviour. Tests performed in neutral gear sought to examine the vehicle's inherent behaviour devoid of gear engagement, yielding essential baseline data. Table A1 summarizes the driving experiments and corresponding details.

Table A1
Summary of experimental tests and parameters.

Test Num	Test Type	Gear	Duration	Num of Datasets	Repetition
1	Runup	G1	40	100	2
2	Coast down	G1	40	100	2
3	Runup	G2	40	100	2
4	Coast down	G2	40	100	2
5	Runup	G3	40	100	2
6	Coast down	G3	40	100	2
7	Runup	G4	40	100	2
8	Coast down	G4	40	100	2
9	Runup	G5	40	100	2
10	Coast down	G5	40	100	2
11	Idle	Neutral	10	25	2

This thorough procedure guarantees that the data required for ML models is both diverse and exact, facilitating the creation of highly accurate transmissibility functions. To reduce uncertainty each experiment was conducted twice under the same conditions. Each dataset was recorded for 0.5 s with a 10 % overlap, maximizing data density and ensuring that even transient phenomena are captured. This comprehensive method establishes a strong basis for analysis and modelling, facilitating reliable outcome.

References

[1] Hastie, T., Tibshirani, R., Friedman, J., & Franklin, J. (2005). The elements of statistical learning: data mining, inference and prediction. *The Mathematical Intelligencer*, *27*(2), 83–85.
[2] Grömping, U. (2009). Variable importance assessment in regression: linear regression versus random forest. *The American Statistician*, 63(4), 308–319.

Data availability

The data materials utilized in this study are subject to confidentiality restrictions and cannot be shared. Consequently, the figures presented in this paper do not include specific y-axis data; instead, scaled arrows are used to represent relevant trends and differences while preserving the confidentiality of the underlying data.

References

[1] Van der Auweraer H, Bianciardi F, Van de Ponseele P, Janssens K. Transfer path analysis innovations for airborne noise problems with focus on pass-by-noise. No. 2014-36-0801. SAE Technical Paper; 2014.

[2] Panda KC. Dealing with noise and vibration in automotive industry. Procedia Eng 2016;144:1167–74.

[3] Oktav A, Anlaş G, Yılmaz Ç. Assessment of vehicle noise variability through structural transfer path analysis. Int J Veh Des 2016;71(1–4):300–20.

[4] van der Seijs MV, De Klerk D, Rixen DJ. General framework for transfer path analysis: history, theory and classification of techniques. Mech Syst Sig Process 2016;68:217–44.

[5] Ye S, Hou L, Zhang P, Bu X, Xiang J, Tang H, et al. Transfer path analysis and its application in low-frequency vibration reduction of steering wheel of a passenger vehicle. Appl Acoust 2020;157:107021.

[6] De Sitter G, Devriendt C, Guillaume P, Pruyt E. Operational transfer path analysis. Mech Syst Sig Process 2010;24(2):416–31.

[7] Almirón JO, Bianciardi F, Corbeels P, Pieroni N, Kindt P, Desmet W. Vehicle road noise prediction using component-based transfer path analysis from tire test-rig measurements on a rolling tire. J Sound Vib 2022;523:116694.

[8] Ortega Almirón J, Bianciardi F, Risaliti E, Corbeels P. Road Noise assessment using component-based TPA for a tire assembly. In: International Congress: SIA-CTTM Automotive NVH Comfort-Quietness Mobility of the Future. SIA; 2018. p. 1–7.

[9] Noumura K, Yoshida J. A method of transfer path analysis for vehicle interior sound with no excitation experiment. Proceedings of FISITA 2006 World Automotive Congress. 2006.

[10] Lohrmann M, Hohenberger T. Operational transfer path analysis: comparison with conventional methods. J Acoust Soc Am 2008;123(5):3534.

[11] De Klerk, D., Lohrmann, M., Quickert, M., & Foken, W. (2009, March). Application of operational transfer path analysis on a classic car. In Proc. DAGA.

[12] Janssens K, Gajdatsy P, Gielen L, Mas P, Britte L, Desmet W, et al. OPAX: a new transfer path analysis method based on parametric load models. Mech Syst Sig Process 2011;25(4):1321–38.

[13] Putner, J., Fastl, H., Lohrmann, M., Kaltenhauser, A., & Ullrich, F. (2012). Operational transfer path analysis predicting contributions to the vehicle interior noise for different excitations from the same sound source. In 41st International Congress and Exposition on Noise Control Engineering, INTER-NOISE, New York City, USA.

[14] Putner, J., Lohrmann, M., & Fastl, H. (2013, June). Contribution analysis of vehicle exterior noise with operational transfer path analysis. In Proceedings of Meetings on Acoustics (Vol. 19, No. 1). AIP Publishing.

[15] Hills E, Mace BR, Ferguson NS. Acoustic response variability in automotive vehicles. J Sound Vib 2009;321(1–2):286–304.

[16] Song D, Hong S, Seo J, Lee K, Song Y. Correlation analysis of noise, vibration, and harshness in a vehicle using driving data based on big data analysis technique. Sensors 2022;22(6):2226.

[17] Chavan, S. (2022, December). Applications of Machine Learning in Automotive Verification and Validation: A Review. In Techno-Societal 2016, International Conference on Advanced Technologies for Societal Applications (pp. 291-303). Cham: Springer International Publishing.

[18] Tsokaktsidis DE, Nau C, Maeder M, Marburg S. Using rectified linear unit and swish based artificial neural networks to describe noise transfer in a full vehicle context. J Acoust Soc Am 2021;150(3):2088–105.

[19] Lee D, Park YY. Transfer path analysis using deep neural networks trained by measured operational responses. J Mech Sci Technol 2023;37(11):5739–50.

[20] Park U, Kang YJ. Operational transfer path analysis based on neural network. J Sound Vib 2024;579:118364.

[21] Tcherniak, D., & Schuhmacher, A. P. (2008). Application of decomposition-based technique in NVH source contribution analysis. Proceedings of ISMA-2008, Leuven, Belgium.

[22] Gajdatsy P, Janssens K, Gielen L, Mas P, Van Der Auweraer H. Critical assessment of Operational Path Analysis: mathematical problems of transmissibility estimation. J Acoust Soc Am 2008;123(5):3869.

[23] Majumder, A., Rahman, M. M., Biswas, A. A., Zulfiker, M. S., & Basak, S. (2022). Stock market prediction: a time series analysis. In Smart Systems: Innovations in Computing: Proceedings of SSIC 2021 (pp. 389-401). Springer Singapore.

[24] Rousson V, Goşoniu NF. An R-square coefficient based on final prediction error. Stat Methodol 2007;4(3):331–40.

[25] Guimaraes, G. P., & Medeiros, E. B. (2007, August). Using transfer path analysis to improve automotive acoustic comfort. In INTER-NOISE and NOISE-CON Congress and Conference Proceedings (Vol. 2007, No. 5, pp. 2498-2506). Institute of Noise Control Engineering.

[26] Sakhaei B, Durali M. Vibration transfer path analysis and path ranking for NVH optimization of a vehicle interior. Shock Vib 2014;2014(1):697450.

[27] International Organization for Standardization. (2023). Acoustics — Measurement of interior vehicle noise (ISO Standard No. 5128:2023). Retrieved from https://www.iso.org/standard/77369.html.